

4DVAR assimilation of SSM/I total
column water vapour in the
ECMWF model

É. Gérard and R. Saunders

Research Department

January 1999

This paper has not been published and should be regarded as an Internal Report from ECMWF.
Permission to quote from it should be obtained from the ECMWF.



Abstract

Special Sensor Microwave Imager radiances have been used to infer a total column water vapour amount using a one dimensional variational retrieval in the ECMWF forecast model. These retrievals are then assimilated using the operational four dimensional variational analysis at ECMWF. The impact of assimilating the total column water vapour on the ECMWF analyses and forecasts is assessed. The primary impact is on the model analysed humidity fields in the Tropics and Southern Hemisphere where 2 to 4% more water vapour is included in the lower troposphere. The addition of moisture in the model also has an impact on the meridional circulation. Small beneficial impacts are seen in the Northern Hemisphere forecast performance at low levels. A case study is presented of the improved forecast of low pressure systems in the Southern Ocean, when SSM/I data are used in 4DVar.

1 Introduction

Radiosonde measurements of water vapour profiles over the oceans are very sparse and even where there are data the accuracy of humidity sensors is limited to 2 to 5% of the relative humidity in the lower troposphere and suffer from a global tendency to underestimate the relative humidity by up to 7% particularly for low temperatures (Balagurov *et al.* 1998). Moreover some sensors do not respond to humidity changes at temperatures lower than -30°C (Schmidlin 1998). Until recently radiosonde measurements were the only data used operationally in numerical weather prediction models for humidity analysis. Radiances from the water vapour channels of the TIROS Operational Vertical Sounder (TOVS) are now assimilated to improve the model's representation of tropospheric humidity but these data are only available in cloud-free areas.

More recently radiances from the Special Sensor Microwave/Imager (SSM/I) on the polar orbiting Defence Meteorology Satellite Program (DMSP) satellites have become available in near real time from the National Oceanic and Atmospheric Administration (NOAA). Radiances from SSM/I, with a field of view less than 50km, offer the possibility to obtain total column water vapour (TCWV) measurements over the ocean in non-precipitating cloudy areas as well as cloud-free areas.

Several NWP centres are using SSM/I TCWV data in data assimilation experiments (Wu and Derber 1994; Ledvina and Pfaendtner 1995; Filiberti *et al.* 1998; Phalippou and Gérard 1996; Deblonde 1999) and have demonstrated benefits in terms of the improved humidity analyses and forecasts. Moreover Aonashi and Shibata (1996) show that assimilating SSM/I TCWV contributes to eliminating model precipitation in observed rain-free areas.

SSM/I TCWV has also been used as an independent measurement to validate the model humidity fields (e.g. Phalippou 1992; Deblonde *et al.* 1997), to demonstrate the impact of model changes for instance assimilation of TOVS radiances (McNally and Vesperini 1996) and to validate a new model cloud scheme (Vesperini 1998).

TCWV from SSM/I radiances can be retrieved using a variety of regression algorithms (e.g. Alishouse *et al.* 1990; Petty 1990; Bauer and Schluessel 1993; Lojou *et al.* 1994). However in common with the initial use of TOVS radiances at ECMWF (Eyre *et al.* 1993) a one dimensional variational retrieval scheme (1DVar) has been developed (Phalippou 1996) to simultaneously

infer TCWV, surface wind speed and cloud liquid water path from SSM/I radiances. This uses the ECMWF 6 hour forecast to provide the first guess profiles. An advantage of the 1DVar retrievals is that they give better coverage in cloudy areas (particularly in the tropics) and for cloud liquid water give values slightly more consistent with the model fields. TCWV is computed from the 1DVar retrieved specific humidity profile and is assimilated globally over sea using the four dimensional variational assimilation system, 4DVar, operational at ECMWF since 25 November 1997 (Rabier *et al.* 1997; Andersson and Järvinen 1999). In the future the direct assimilation of SSM/I radiances in 4DVar could be considered as is the case for TOVS but the inclusion of cloud liquid water in the control vector makes this more complex.

This technical memorandum is structured as follows. Section 2 briefly describes the SSM/I instrument and the data used for the experiments and section 3 describes the 1DVar retrieval. Section 4 describes how the data were assimilated in 4DVar and sections 5 and 6 show the impact of the TCWV data on the analyses and forecasts respectively.

2 Characteristics of SSM/I

2.1 Description of the instrument

The SSM/I is a seven-channel radiometer which operates in both vertical (V) and horizontal (H) polarizations at 19.35, 37.0 and 85.5 GHz and at 22.235 GHz where only the V polarization is available. Six SSM/I's have been launched thus far on DMSP satellites: first in June 1987 (F8), and most recently in April 1997 (F14). The SSM/I consists of an offset parabolic antenna with a diameter of about 60 cm and a total power radiometer. The scanning is conical with an angle of 45°. DMSP satellites are in a polar orbit at an altitude of about 830 km, resulting in a 53.1° incidence angle and a 1400 km swath. The effective fields of view (EFOVs) of the half-power beamwidths of the SSM/I antenna are given in Table 1. The EFOVs account for the integration time of the radiometer. The pre-launch specification for the SSM/I radiometric sensitivities ($Ne\Delta T$ s) is also given in Table 1. A detailed description of the SSM/I instrument can be found in Hollinger *et al.* (1990). The SSM/I data used in this study came from the DMSP-F13 satellite.

The orbit-by-orbit geolocated SSM/I brightness temperatures are transferred from the NOAA's National Environmental Satellite, Data and Information Service (NESDIS) to the UK Meteorological Office in Bracknell which sends them on in near real time to ECMWF.

Table 1: SSM/I effective fields of view (EFOV) and radiometric sensitivities ($Ne\Delta T$).

Frequency (GHz)	19.35	22.235	37.0	85.5
Polarization	V & H	V & H	V & H	V & H
EFOV (km)	69 × 43	60 × 40	37 × 28	15 × 13
$Ne\Delta T$ (K)	0.8	0.8	0.6	1.1

2.2 Brightness temperature bias correction

The SSM/I measured brightness temperatures are used as observations in the 1DVar retrieval jointly with the ECMWF first guess to provide the SSM/I 1DVar products (see section 3). As the 1DVar method relies on the accuracy of the radiative transfer model any bias in the model or in the observed radiances can lead to biased products. The brightness temperature bias correction aims at minimizing the global mean difference between observed and computed radiances for some collocated ground truth. The ECMWF collocated first guess may constitute a ground truth, but it has to be unbiased. The following hypotheses have been adopted to ensure this:

- the model sea surface temperature, wind speed and the temperature profile are assumed globally unbiased;
- the biases, assumed to be independent of the presence of cloud, are computed only under clear conditions;
- as the ECMWF model has a dry bias especially in the Tropics (Phalippou and Gérard 1996; Vesperini 1998), the vertical humidity structure of the first guess is rescaled in such a way that globally the model TCWV is equal to the SSM/I TCWV retrieved from the algorithm developed by Alishouse *et al.* (1990). This algorithm was developed from collocated radiosondes and SSM/I observations and reflects the global mean truth in as much as radiosondes do.

The estimated brightness temperature biases, reported in Table 2, were computed from a representative set of first guess fields for a period of one day (9000 observations met the criteria listed above). They are added to the SSM/I observed brightness temperatures before the minimisation in 1DVar.

Table 2: Mean bias correction in the vertical and horizontal polarizations.

Frequency (GHz) and Polarization	19V	19H	22V	37V	37H	85V	85H
Mean bias (K)	-1.55	-1.60	-1.06	0.38	-1.34	2.20	1.75

The brightness temperature bias correction processed and used in our study is inherent to the data source. A study by Ritchie *et al.* (1998) concluded that there are no significant differences between the DMSP-F11 antenna temperatures obtained from NESDIS and FNMOC (Fleet Numerical Meteorology and Oceanography Center). However another study (Cloud Retrieval Validation project, Offiler *et al.* 1998) showed that the differences are significant in terms of brightness temperatures. For instance the DMSP-F13 interchannel root mean square differences between NESDIS and FNMOC data range typically from 0.1 to 1.3 degK with the highest values

obtained in the 22V and 37H channels. These statistics were obtained from comparisons in the area bounded by 50°N - 60°N and 10°W - 10°E on 16 October 1996 and 1 January 1997. These brightness temperature differences are of the same order of magnitude as the bias corrections, emphasizing that the bias correction is dependent on the data source.

The mean global radiance biases for all the SSM/I channels are monitored daily and to date for DMSP-F13 have been very stable.

3 SSM/I 1DVar retrievals

SSM/I 1DVar is a method for retrieving the atmospheric humidity profile, the surface wind speed and the cloud liquid water path from SSM/I brightness temperature observations over the oceans. The geophysical parameters are estimated simultaneously following the theory of non-linear optimal estimation (Rogers 1976), and are therefore the best set of parameters that explain the observed brightness temperatures, while being consistent with the available *a priori* information given by the ECMWF first guess. A detailed description of the method is given by Phalippou (1996). Since then a few minor changes have been made. A brief summary of the method is described below.

3.1 Method

We define \mathbf{x} as the control variable, which is comprised of the natural logarithm of the specific humidity profile on 15 fixed pressure levels between 300 and 1000 hPa, the surface wind speed and the cloud liquid water path.

We seek the best estimate of \mathbf{x} knowing the *a priori* or background vector \mathbf{x}^b given by the ECMWF first guess and the coincident satellite observation vector \mathbf{y}^o . We denote by H the forward operator mapping the control variable \mathbf{x} into the observation space; H is the radiative transfer model which computes the brightness temperatures corresponding to the control variable \mathbf{x} . A description of the fast radiative transfer model is given in Phalippou (1993) which uses transmittances computed by the Liebe (1989) microwave transmittance model. The observation operator H also includes an inverse spectral transform to go from spectral to grid point space and spatial interpolations from the model fields to the measurement locations: a 12-point bicubic horizontal interpolation gives vertical profiles of model variables at observation points, except for liquid water content which is obtained from a bilinear interpolation to avoid over smoothing of the first guess field. The surface fields are interpolated bilinearly to avoid spurious maxima. A vertical extrapolation of the first guess fields to 40 fixed pressure levels up to 0.1 hPa is also performed, as required by the radiative transfer model. Only the 15 lowest levels are used in the 1DVar minimisation, as the moisture we intend to modify with the SSM/I observations is mostly concentrated below 300 hPa.

When the errors in the observations and the *a priori* information have Gaussian distributions and are uncorrelated, then the cost function J composed of a background and an observation term is given by:

$$J(\mathbf{x}) = (\mathbf{x} - \mathbf{x}^b)^T \mathbf{B}^{-1} (\mathbf{x} - \mathbf{x}^b) + (\mathbf{y}^o - H(\mathbf{x}))^T \mathbf{R}^{-1} (\mathbf{y}^o - H(\mathbf{x})) \quad (1)$$

where \mathbf{B} and \mathbf{R} are the expected background and observation error covariance matrices respectively. The superscript T denotes the matrix transpose and -1 the matrix inverse. By definition, the best estimate of \mathbf{x} corresponds to the maximum of the probability density function and is found by minimising the cost function J .

A modified Newtonian iteration scheme with bound constraints on the control variable \mathbf{x} is used in this study. The lower bounds on wind speed and cloud liquid water path are set to 0.1 m s^{-1} and $10^{-4} \text{ kg m}^{-2}$ respectively. The use of the logarithm of the specific humidity alleviates the lower bound problem but the humidity supersaturation needs to be controlled by adding a penalty term J_c to the background and observation terms in Equation 1. It is defined as the summation of the supersaturation intensity on the 15 levels where the specific humidity at level i (q_i) during the minimisation is greater than or equal to the background specific humidity at saturation at the same level (q_i^{sat}):

$$J_c = c \sum_{i=1}^{15} \max(0., (\ln(q_i) - \ln(q_i^{sat}))^3) \quad (2)$$

where c is a constant tuned such that a supersaturation up to 7% is permitted, which corresponds to a 1 degK first guess temperature profile error. The value of c in the current 1DVar is 8000.

3.2 Error Covariance Matrices

The observation errors are composed of errors in the brightness temperature observed by the radiometer, errors in the brightness temperatures simulated through the forward model and errors arising from interpolation of the model fields to the observation point. The errors related to the instrument are assumed to be uncorrelated, i.e. the observation error covariance matrix is diagonal and its elements are set to the Ne Δ Ts of the instrument (see Table 1). The radiometric noise is not the main factor in the error budget because it is much lower than the errors assumed in the forward model. As the forward model errors are also assumed to be uncorrelated, the \mathbf{R} matrix is diagonal and the square root of its diagonal terms are set to 2 degK for all the channels except for the 85.5 GHz channels where the errors are set to 3 degK in order to account for the higher Ne Δ T (see Table 1) and greater sensitivity to cloud effects not simulated.

The elements of the background error covariance matrix related to specific humidity have been derived from the \mathbf{B} matrix used in the operational TOVS-1DVar scheme (Eyre *et al.* 1993) and do not depend on the background profile itself. The background error correlation matrix given in Phalippou (1996) has been updated (see Table 3) in order to account for the different number of vertical levels for specific humidity. A 2 m s^{-1} first guess error is assumed for wind speed as suggested by a comparison between ECMWF first guess wind field and ERS-1 scatterometer measurements (Stoffelen and Anderson 1994). The cloud liquid water path background error is set to 0.2 kg m^{-2} which represents a weak constraint allowing the observations to mainly influence the retrieved cloud liquid water path.

Table 3: Background error correlation matrix and standard deviations for 1DVar.

Correlation matrix of background error (*100)																		
X	PRES																	
ln(q)	300	1	100															
ln(q)	350	2	51	100														
ln(q)	400	3	44	88	100													
ln(q)	430	4	26	60	69	100												
ln(q)	475	5	18	47	54	74	100											
ln(q)	500	6	18	49	56	82	87	100										
ln(q)	570	7	11	29	32	45	49	56	100									
ln(q)	620	8	10	23	26	36	39	45	73	100								
ln(q)	670	9	9	20	22	30	33	38	71	75	100							
ln(q)	700	10	10	21	22	32	34	39	80	85	88	100						
ln(q)	780	11	12	17	19	23	24	28	49	51	52	59	100					
ln(q)	850	12	13	16	18	19	20	23	37	38	39	44	74	100				
ln(q)	920	13	14	11	11	13	13	15	22	22	22	24	39	46	100			
ln(q)	950	14	15	9	7	9	8	9	13	13	12	13	21	17	66	100		
ln(q)	1000	15	14	10	10	15	15	17	19	18	17	19	29	36	64	63	100	
WS		16	0	0	0	0	0	0	0	0	0	0	0	0	0	0	100	
LWP		17	0	0	0	0	0	0	0	0	0	0	0	0	0	0	100	
	Element	1	2	3	4	5	6	7	8	9	10	11	12	13	14	15	16	17
Standard deviation of background error (*100)																		
		74	74	70	67	70	63	62	66	70	63	56	50	53	65	44	200	20

X: Control variable

PRES: Fixed pressure (hPa)

q: Specific humidity (kg kg^{-1})

WS: Surface wind speed (m s^{-1})

LWP: Cloud liquid water path (kg m^{-2})

3.3 Quality control within SSM/I 1DVar

Since 24 February 1998 the SSM/I 1DVar products have been derived within the ECMWF operational model run once every six hours. The SSM/I brightness temperatures are collected over a 6-hour window centred on the synoptic times (00/06/12/18 UTC). The first guess is derived from the 4DVar assimilation system.

An *a priori* quality control consists of keeping observations only over the ocean by checking that the model land fraction is less than 1 % and the SSM/I surface type index provided with the observed brightness temperatures is water. The lowest model surface temperature allowed is set to 273.14 degK, to avoid sea-ice. Finally the presence of all the observed brightness temperatures in each report is checked as well as their value to range within the interval 70 to 320 degK. A sampling of 1 out of 5 points across the scan and every fifth scan line (125 km spacing) is performed to allow the computations to be carried out without significantly impacting the time taken to complete the analysis. As a result of this thinning only a few thousand SSM/I observations are processed, typically from 4000 to 8000 every six hours depending on the orbit positions relative to land.

An *a posteriori* quality control is applied to the three products simultaneously. The 1DVar minimisation has to be successful and the model first guess must not be too far from the observation in terms of brightness temperature. The second term of the right side of Equation 1 (observation cost function) has to be lower than 10.

Fig. 1 shows an inter-comparison of TCWV derived from the ECMWF first guess, the SSM/I 1DVar method and the Alishouse regression from 27 November 1997 at 00, 06, 12 and 18 UTC.

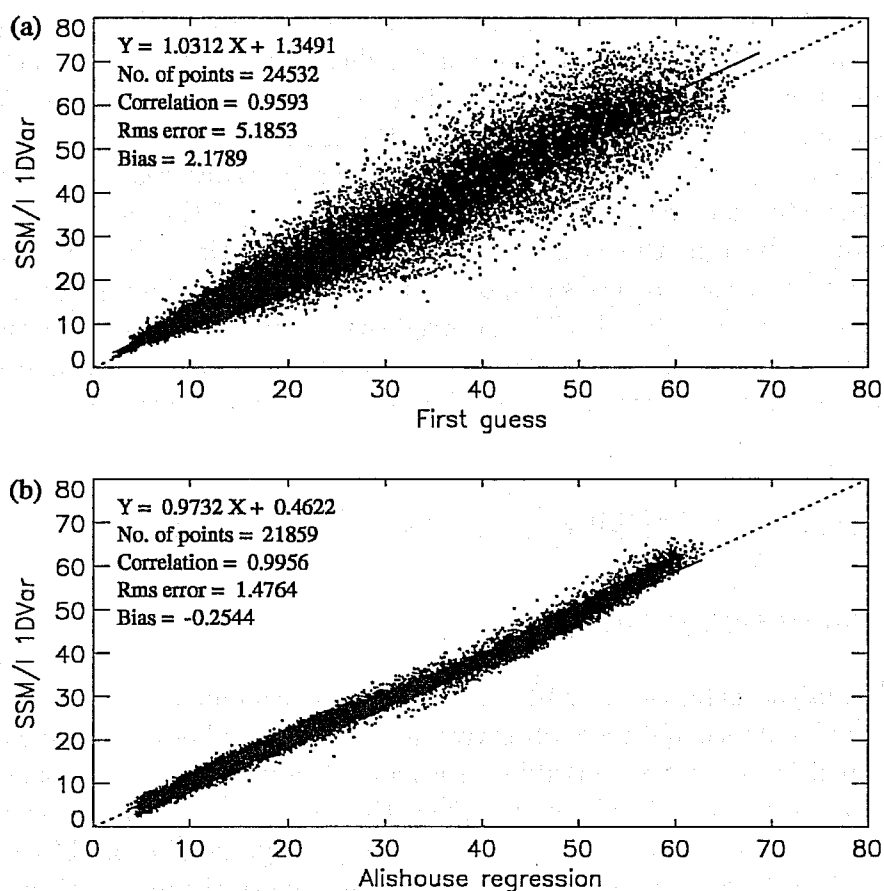


Figure 1: SSM/I 1DVar retrieved TCWV compared to TCWV retrieved from (a) the first guess, (b) the Alishouse regression on 27 November 1997. Units are in kg m^{-2} .

It is clear that the SSM/I 1DVar TCWV retrievals are greater than the first guess TCWV values for any range of values (Fig. 1(a)). The model's moisture deficit can be found at any latitude band (see Section 5). It can reach in extreme cases 50% relative to SSM/I 1DVar. Vesperini (1998) found similar results in a comparison over a 2-week period of TCWV derived from the ECMWF operational analysis and the Alishouse *et al.* (1990) algorithm, but the underestimation only occurred in the Tropics. The same study highlighted the tendency of the model, as it was in 1994, to be too moist in the "dry tongues" located off the western coasts of subtropical continents and in mid-latitudes. The biases associated with the tropical regions and the subsidence areas are still present in the current ECMWF model but to a lesser extent due to the assimilation of TOVS radiances (McNally and Vesperini 1996). As for the mid-latitude biases the model changes between 1994 and 1998 have decreased the moisture field, so that it is now underestimated, particularly in the Southern Hemisphere, when compared with SSM/I 1DVar TCWV retrievals. Three model changes are candidates to explain this new behaviour: Optimal Interpolation has been replaced by 3DVar and 4DVar successively, the diagnostic cloud scheme was replaced by the prognostic cloud scheme and a new model physics package has been implemented (Gregory *et al.* 1998).

When 1DVar TCWV is compared to Alishouse TCWV there is as expected a good agreement between the retrievals (Fig. 1(b)). However a small overestimation and underestimation of Alishouse TCWV at respectively low and high water vapour content is evident. Such biases have already been reported by Alishouse *et al.* (1990), Petty (1990), Colton and Poe (1994), Phalippou (1996) and Deblonde and Wagneur (1997). They are due to the intrinsic nonlinearity of the retrieval problem which is difficult to handle when a regression-type method is used. A modified version of the Alishouse algorithm has been developed by Petty (see Colton and Poe 1994), involving a cubic polynomial correction of the initial estimate which mainly corrects the extreme values of TCWV. Note finally that 1DVar provides reasonable TCWV in the areas which are detected as precipitating by Alishouse (11% of the points), suggesting that the method is more robust in the presence of rain contamination. The fact that 1DVar is in better agreement with the Alishouse algorithm than with the first guess means that the 1DVar retrievals are more correlated with the brightness temperature observations than with the model field. Even though the retrievals are partly derived from the first guess, they can be considered as independent observations, which justifies their assimilation into the model.

4 Assimilation of SSM/I TCWV in 4DVar

4.1 4DVar analysis system

The ECMWF analysis is based on a 4DVar assimilation system (Rabier *et al.* 1997). 4DVar seeks for an optimal balance between observations and atmospheric dynamics by finding a model solution which is as close as possible, in a least square sense, to the background information and the observations available over a given time period. It is being used at ECMWF in its incremental formulation which comprises running a high-resolution T319 model (triangular truncation at total wave number 319) with the full physical parametrisation package to compare the atmospheric state with the observations and a low resolution model (T63) with simplified physics to minimise the cost function. A “2-update” configuration is used in the minimisation: 50 iterations are performed without physics and, after updating the trajectory at high resolution, 20 iterations are performed with physics.

A preliminary study to assimilate TCWV was previously made at ECMWF (Filiberti *et al.* 1998), but the physics involved in the T63 minimisation was very simplified (horizontal diffusion, a simple surface drag and a vertical diffusion scheme). It now also includes radiation, surface processes, sub-grid scale orography, turbulence in the planetary boundary layer, moist deep and shallow convection and cloud formation and dissipation.

4.2 Experimental design

The introduction of a new type of observation in 4DVar consists of adding a term in the observation cost function; in the case of TCWV the additional term $J_{SSM/I}^o$ measuring the misfit of the model to SSM/I data is written in the form:

$$J_{SSM/I}^o = \frac{1}{2} \sum_{i=0}^n \frac{(y^{mod} - y^o)^2}{\sigma_0^2} \quad (3)$$

where y^o is the SSM/I TCWV observation and σ_0^2 its related error, y^{mod} is the model state forecast at observation time t_i mapped into the observation space, i being the time index between the beginning and the end of the 6-hour assimilation period. The model operator which converts the model variables into TCWV is obtained with a vertical integration of specific humidity:

$$y^{mod} = \frac{1}{g} \int_0^{p_s} q(p) dp \quad (4)$$

where g is the gravitational constant (m s^{-2}), $q(p)$ is the specific humidity (kg kg^{-1}) at atmospheric pressure p (Pa) and p_s is the surface pressure. The adjoint of this operator is used in the computation of the gradient of $J_{SSM/I}^o$ with respect to the control variable.

4.3 TCWV observation error

The observation error for SSM/I TCWV can be estimated objectively as shown by Rodgers (1976) and empirically based on radiosonde collocations. It is interesting to compare both estimates. For the objective error estimation it can be shown that the analysis error covariance matrix \mathbf{A} of the control variable \mathbf{x} can be approximated by the expression:

$$\mathbf{A}(\mathbf{x}) = (\mathbf{B}^{-1} + \mathbf{H}(\mathbf{x})^T \mathbf{R}^{-1} \mathbf{H}(\mathbf{x}))^{-1} \quad (5)$$

where \mathbf{R} is the expected observation and forward model error covariance matrix, \mathbf{B} the background error covariance matrix and \mathbf{H} is the Jacobian matrix, i.e. its elements are the partial derivatives of the simulated brightness temperatures with respect to the control variable \mathbf{x} . The analysis or *a posteriori* error variances of the estimate of \mathbf{x} are given by the diagonal elements of \mathbf{A} . The TCWV analysis error variance is obtained by vertically integrating the analysis error variances related to specific humidity and can be expressed as the sum of two terms:

$$\sigma_a^{-2} = \sigma_b^{-2} + \sigma_o^{-2} \quad (6)$$

where σ_b and σ_a are the standard deviations of the *a priori* and *a posteriori* errors respectively of TCWV. σ_a can be interpreted as the accuracy which would result from a minimum variance estimator using a background error of σ_b and an independent TCWV measurement with an accuracy of σ_o . As the objective TCWV accuracy σ_a depends on \mathbf{x} , σ_a is evaluated for various atmospheric and surface conditions - hereafter called atmospheric profiles - derived from four consecutive ECMWF first guess fields. Only profiles over the ocean have been selected and a 125 km sampling has been applied to reduce the horizontal model correlations. These profiles span almost the whole range of weather conditions over ocean; the range of TCWV, wind speed and cloud liquid water path for these profiles is respectively 1-70 kg m^{-2} , 0-31 m s^{-1} and 0-1.6 kg m^{-2} . The objective accuracy of SSM/I TCWV, presented in Fig. 2, ranges from 1 to 3 kg m^{-2} while the *a priori* background TCWV error derived from the \mathbf{B} matrix presented in Section 3(b) varies between 1 and 29 kg m^{-2} for a dry (2 kg m^{-2}) and a tropical (70 kg m^{-2}) humidity profile. Fig. 2 shows the TCWV first guess accuracy computed from the operational 4DVar \mathbf{B} matrix for specific humidity (Rabier *et al.* 1998) on the same atmospheric profile dataset. The objective TCWV accuracy is smaller than the 4DVar background error, except for dry profiles.

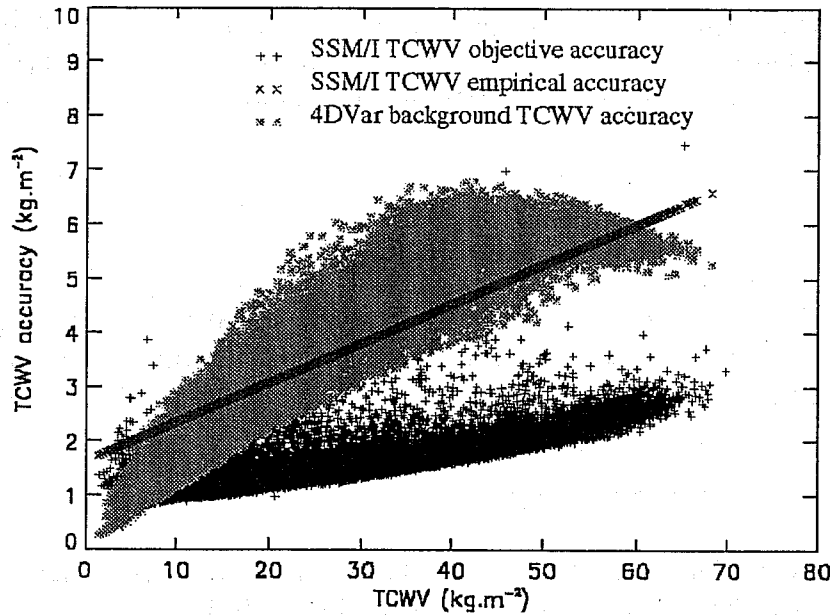


Figure 2: TCWV accuracies for colocated SSM/I TCWV and first guess fields on 28 November 1997 (27721 data).

If TCWV observations were assimilated in 4DVar with an accuracy set to the objective value derived above the analysis would be strongly influenced by the observations along the orbits and by the model fields in the SSM/I data-free areas between the orbits. The length scale of the horizontal structure function for specific humidity of about 250 km in the troposphere (Rabier *et al.* 1998) could not prevent gradients appearing in the vicinity of the edge of the orbits, because of the dry bias between the model field and the observation (see Section 3(c)).

The objective TCWV accuracy can be underestimated due to errors not accounted for in the measurements or forward model and there is evidence for this in comparisons of SSM/I retrieved TCWV with radiosondes (Alishouse *et al.* 1990). Hence a pragmatic approach has been adopted where the TCWV observation errors have been redefined to have a similar order of magnitude to those found with the radiosonde collocations. The TCWV observation error (σ_o) specified in the 4DVar assimilation is empirically defined as a linear function of the TCWV observation (y^o) to approximately fit the radiosonde estimations of SSM/I TCWV error as described in Phalippou and Gérard (1996). The function used is:

$$\sigma_o = 7.27 \cdot 10^{-2} y^o + 1.63 \quad (7)$$

This formulation results in errors similar to the first guess background errors as shown in Fig. 2 so that the first guess is not too strongly modified by the observations along the orbits.

4.4 Thinning and quality control

A second thinning is performed on the 125 km-sampled SSM/I products set before the assimilation for the following reasons. As the 19 to 85 GHz channels are all used to derive

TCWV, the spatial resolution of SSM/I TCWV is in the range 13-70 km (see Table 1). Since the spatial sampling of these channels is every 25 km, horizontal correlations between the errors of two adjacent measurements can be expected and they should be accounted for in the assimilation system. Secondly as the truncation in the 4DVar minimisation is currently performed at wave number 63 (T63), the assimilation itself cannot resolve scales smaller than 210 km. A reasonable compromise between observation coverage and the assumption of no horizontal error correlations is a sampling to 250 km in distance between adjacent observations. As a consequence the 1DVar TCWV dataset is thinned by a factor 4, i.e. about 1000 to 2000 observations from one satellite assumed to be horizontally uncorrelated are assimilated during a 6-hour time period.

The main quality control checks are performed within the 1DVar processing (see Section 3(c)) which prevent any suspect data from reaching the 4DVar assimilation. However as for any observation used in 4DVar, SSM/I 1DVar TCWV are checked within the variational analysis itself through the variational quality control (VarQC) presented in Andersson and Järvinen (1999). The VarQC parameters for SSM/I 1DVar TCWV data are 40 % for the gross error probability and $6\sigma_o$ for the flat distribution interval centered at zero.

4.5 Assimilation and forecast experiments

In order to assess how the use of SSM/I 1DVar TCWV influences the analysis and the forecast, two sets of assimilation experiments have been performed in the 4DVar assimilation system with the T213L31 configuration (triangular truncation at total wave number 213 and 31 model levels sampling the atmosphere between the surface and 10 hPa) for the periods 15 May to 31 May 1997 and 28 November to 15 December 1997, referred to as May'97 and Dec'97 respectively in the rest of the text.

For both periods, assimilation cycles were performed without SSM/I data (Control) and with the addition of SSM/I 1DVar TCWV data (Experiment). In terms of humidity observations the Control experiments assimilated SYNOP and SHIP 2-metre relative humidity data, radiosonde specific humidity profiles below 300 hPa and TOVS cloud-cleared radiances. The Experiment consisted of including SSM/I 1DVar TCWV data with these other observations following the method described in the previous subsections.

The initial data taken from the operational run six hours before the beginning of the assimilation periods were computed using a previous model version prior to the new physics package (Gregory *et al.* 1998) in both cases and before 4DVar for the May'97 experiment. A series of 10-day forecasts were launched once a day from the 12 UTC analyses.

5 Analysis impacts

5.1 Impact on TCWV

The time series of TCWV over the global area, the Northern Hemisphere, the Tropics and the Southern Hemisphere derived from first guess and analysis for the Experiment and the Control of the May'97 period are given in Fig. 3.

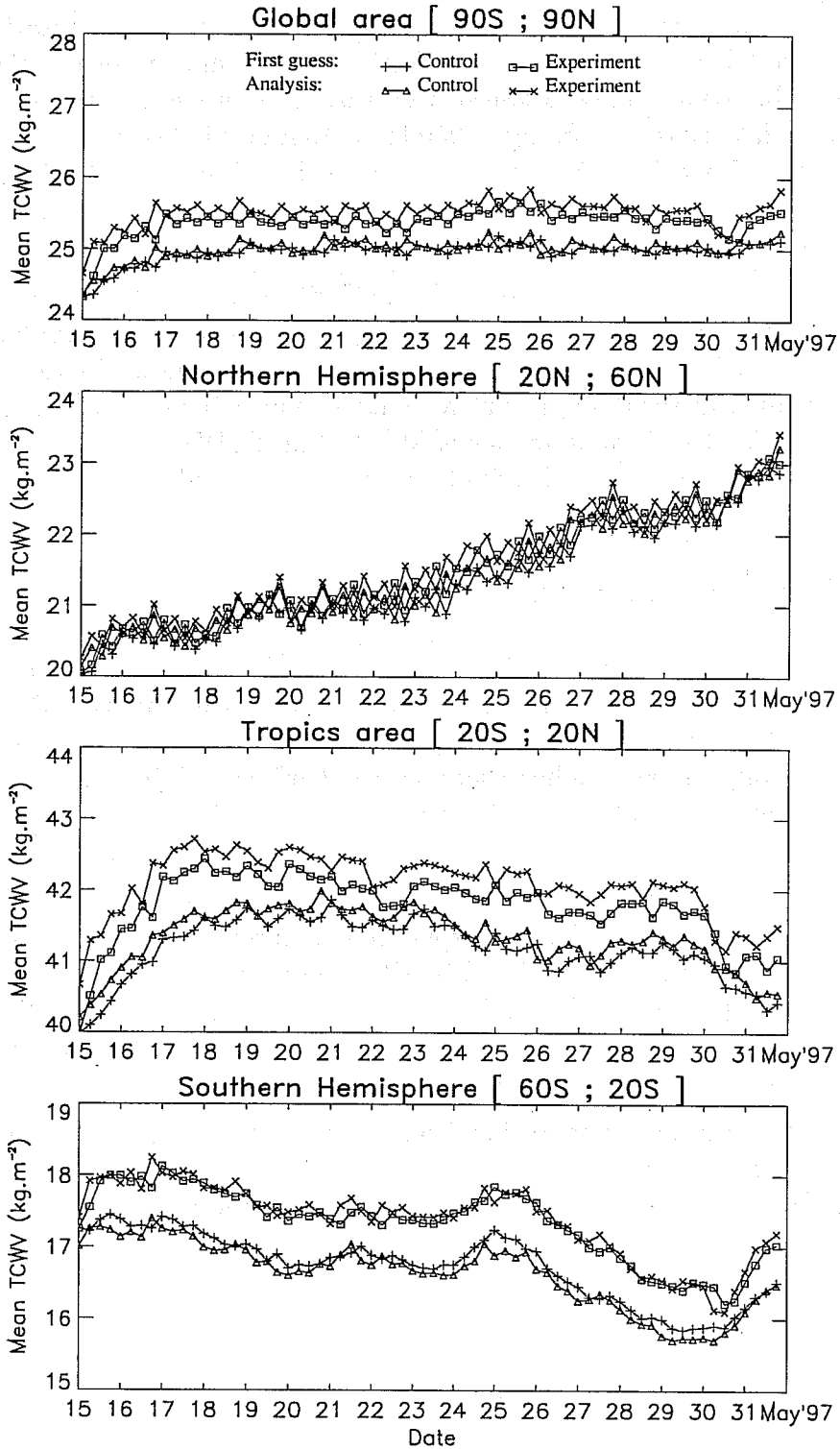


Figure 3: Time series of TCWV derived from first guess and analysis for the Control and the Experiment over the May'97 period and for different latitude bands.

Both experiments start from the same initial data so that the first guesses are identical at the beginning of the assimilation period. The sudden increase of moisture in both experiments during the first four days in the Tropics seems to be related to the progressive adaptation of the 4DVar system to the initial 3DVar atmospheric state. For this reason the first four days of the May'97 period have not been used in the studies that follow. Note that such a moisture spin up is not evident for the Dec'97 experiments, as the runs started from 4DVar fields.

The difference between analysis and first guess, hereafter called increment, shows the impact of the observations in the assimilation. The data used in the Control experiment have a tendency to moisten the atmosphere in the Tropics and slightly dry it in the Southern Hemisphere. The TCWV increments of the Experiment are globally positive throughout the assimilation particularly in the Tropics. According to the background error covariance matrix for specific humidity, two relative maxima characterize the vertical profile of specific humidity increments: the first one in the vicinity of 800 hPa and the second one close to the surface as shown in Fig. 4. The increments for both experiments do not have the same intensities but the same sign when maps of time averaged TCWV increments are compared, showing that there is no conflict on average between TOVS and SSM/I observations. However a few negative mean increments in the Control are found in some places over the Southern Hemisphere ocean where the Experiment analysis does not differ from the first guess on average, which explains the slight negative mean increment in the Control persisting throughout the assimilation period. This is due to the fact that the TOVS and SSM/I instruments are not sensitive to the same vertical layers: mainly upper troposphere for TOVS, lower troposphere for SSM/I and the TOVS provides observations only in cloud-free drier regions.

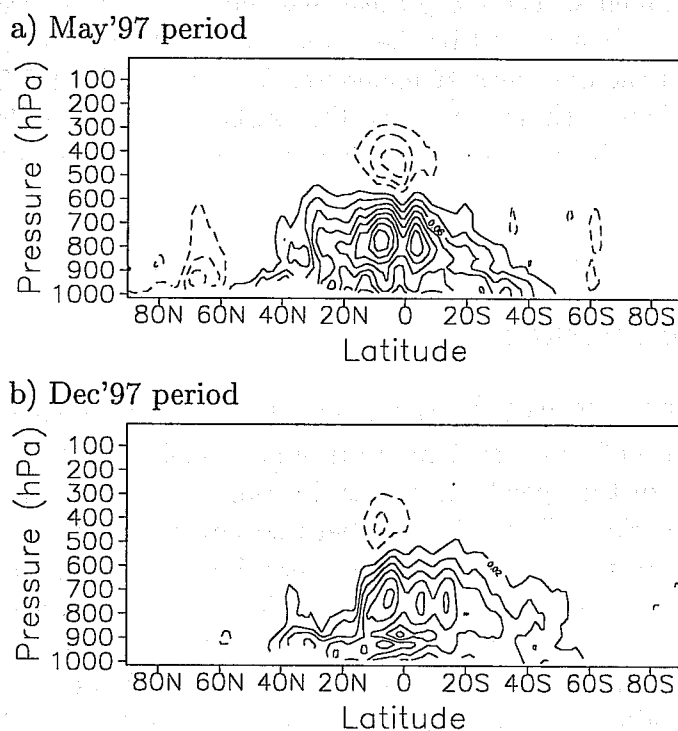


Figure 4: Zonal mean of specific humidity increments in the Experiment averaged over the (a) May'97 and (b) Dec'97 periods and over longitude. The contour interval is 0.02 g kg^{-1} with solid contours representing a moistening (positive values) and dashed ones a drying (negative values) in the analysis.

The positive TCWV increments should decrease during the experiment if the assimilation and short-range forecast processes were optimal. However the constant need to add moisture at each assimilation cycle especially in the Tropics reveals that only part of the moisture is kept by the system during the following six hours. The loss of moisture between one analysis and the following first guess in the Experiment as well as in the Control can be explained by the conversion of this moisture into precipitation in the 6-hour forecast run, as described in section 6.

As a result of the positive increments in the Experiment with SSM/I data over the May'97 period, the Experiment analysis has globally 2% more water vapour than the Control analysis, and the biggest relative TCWV increase is found in the Southern Hemisphere (4.5% increase) followed by the Tropics (1.8% increase) and the Northern Hemisphere (0.7% increase). The Dec'97 Experiment analysis is also characterised by an increase of its specific humidity: 1.7% global increase, 3.9% in the Southern Hemisphere, 1.9% in the Tropics and 1.2% in the Northern Hemisphere.

The TCWV mean fields resulting from the time average of the analysis with and without SSM/I TCWV during the Dec'97 period are compared in Fig. 5. The biggest impact of SSM/I data on the TCWV analysis occurs almost everywhere over the Tropical and the Southern oceans down to approximately 50°S, corresponding to the austral summer polar sea-ice edges, south of which SSM/I TCWV retrievals are not performed. These latitude bands correspond to areas where conventional observations of humidity suffer from sparse coverage and poor temporal resolution, which is not the case in the Northern Hemisphere.

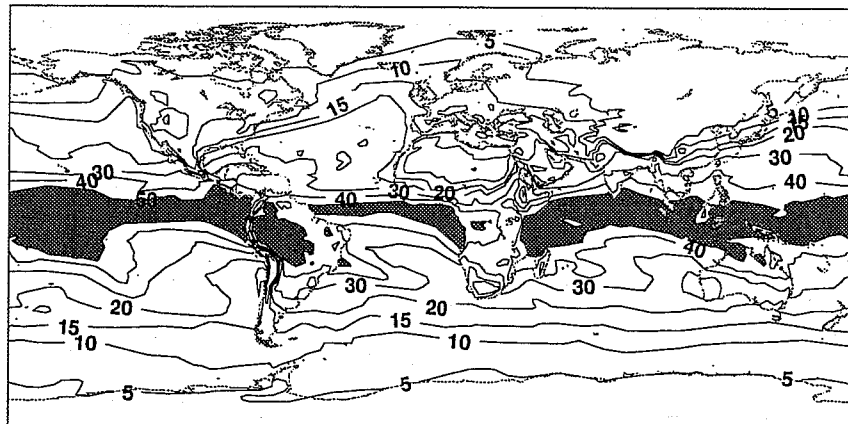
The SSM/I data moistens the analysis, except in the dry tongues located off the western coasts of subtropical continents. These dry areas associated with the descending branch of the Hadley Circulation are poorly analysed by the model without SSM/I in that they are generally too moist particularly in the Southern Hemisphere. The use of SSM/I TCWV data helps to reduce this model moist bias in these areas, and this is also true for the May'97 period, but to a lesser extent, in agreement with a better analysis in the austral winter (McNally and Vesperini 1996).

5.2 Impact on temperature

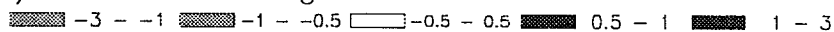
The use of SSM/I 1DVar TCWV in 4DVar also has an impact on the temperature field. Fig. 6 shows the difference of analysed temperature at model level 24 (770 hPa) which corresponds to the maximum of the specific humidity increment between the Experiment and the Control for the Dec'97 period. There is a global temperature increase of 0.11 degK due to SSM/I but the warming in the Tropics and Southern Hemisphere, generally associated with a moistening, can also be due to a drying, for example along the western Peruvian coast (see Fig. 5). As the analysis of specific humidity is univariate, the modification of the temperature field is due to the way the model physics is affected by the analysis moistening. However the temperature increase can also be due to a change in the dynamical circulation (see Section 5(c)).

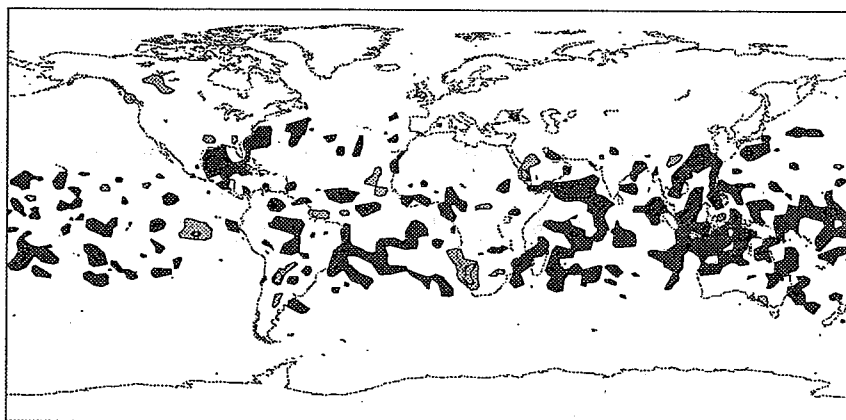
The May'97 period is also characterised by a warming at model level 24 when SSM/I data are used, but it covers wider areas in the Southern Pacific and Indian Ocean, and spreads into the Southern Atlantic as well. On average over the May'97 period the warming in the analysis is of the same order of magnitude (0.14 degK) as over the Dec'97 period (0.11 degK).

a) Mean value: 24.70 kg m^{-2}

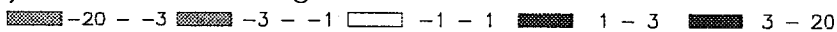


b) Mean value: 0.15 kg m^{-2}


 -3 - -1 -1 - -0.5 -0.5 - 0.5 0.5 - 1 1 - 3



c) Mean value: 0.42 kg m^{-2}


 -20 - -3 -3 - -1 -1 - 1 1 - 3 3 - 20

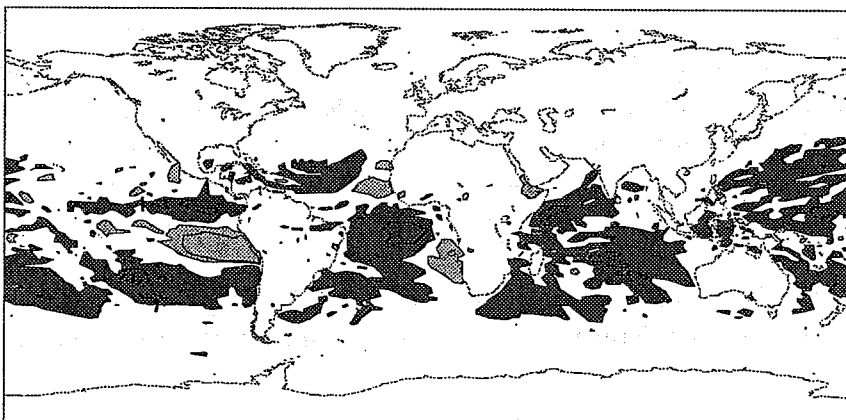


Figure 5: Mean values computed over the Dec'97 period: (a) TCWV from the Experiment analysis; (b) TCWV increments for the Experiment; (c) TCWV difference between the Experiment and the Control analyses. Units are in kg m^{-2} and mean field values are indicated at the top of each panel.

The global warming in the Tropics and Southern Hemisphere also occurs at higher levels, generally associated with a moistening of the atmosphere at the same level. For instance in the Tropical Pacific the warming in the analysis for both periods can locally reach 0.6 degK at level 10 (200 hPa) with a 60% average specific humidity increase over each of the two assimilation periods.

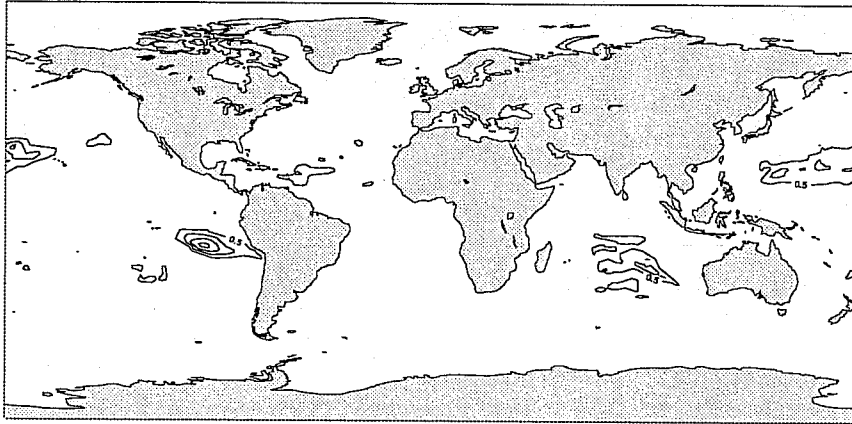


Figure 6: Difference of model level 24 (around 770 hPa) temperature between the Experiment and the Control analyses on average over the Dec'97 period. The contour intervals are 0.5 degK. All the contours represent a positive difference. The global mean difference is 0.11 degK.

5.3 Impact on the dynamics

The changes in the humidity analysis are associated with marked changes in the meridional circulation; Fig. 7 shows the zonal mean vertical velocity field of the Experiment and the Control analyses for the May'97 period. The general moistening by TCWV is accompanied by a more intense area of mean ascent at the equator (up to 25% increase in the vicinity of 400 hPa), and by a strengthening of the subsidence motions between 200 and 600 hPa over the latitude bands 10°S - 30°S (up to 7 % increase) and 15°N - 30°N (up to 20 % increase). The effect of assimilating SSM/I TCWV is to increase the Hadley circulation, but no impact is found on the position and the width of the associated cells. The stronger Hadley circulation is also noticeable in the Dec'97 period, but the biggest impact of SSM/I on the downward motion is then found in the Southern Hemisphere and the upward motion is strengthened in the northern ascent branch by up to 30 % on average.

As a result of the intensification of the Hadley cell the cloud liquid water content is increased by 5 to 8 % along the ascending branch and decreased by 13 to 17 % in the subsidence cells at about 700 hPa. Apart from this modification of the cloud liquid water field related to convection, an increase of the liquid water content at about 800-900 hPa between 40°S and 60°S of latitude is also seen. It is likely to be caused by the development of stratiform clouds in relation to the increase of moisture over the same area (see for instance Fig. 5 for the Dec'97 period).

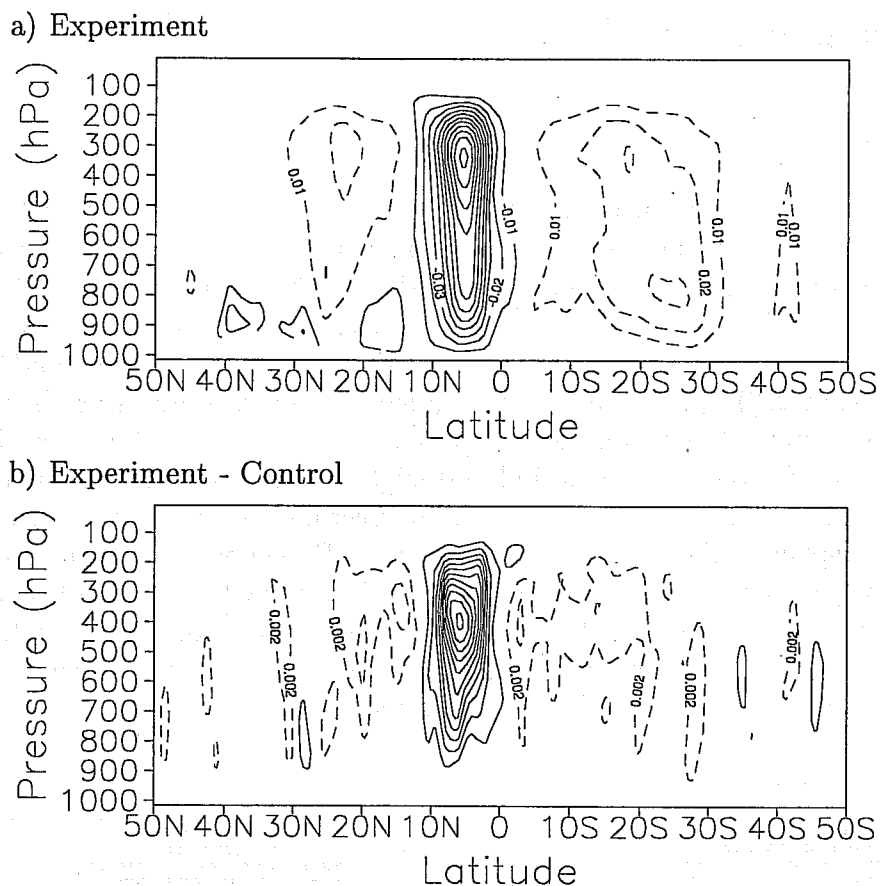


Figure 7: Zonal mean of analysis rate of change of pressure (dP/dt) for (a) the Experiment averaged over the May'97 period and over longitude and (b) the difference between the Experiment and Control. The contour interval is (a) 0.01 Pa s^{-1} with solid contours representing upward motion (negative values) and dashed contours representing downward motion (positive values) and (b) 0.002 Pa s^{-1} with solid contours representing negative differences and dashed contours representing positive differences. The abscissa is the latitude in degrees and the ordinate the model pressure in hPa.

5.4 Fit of first guess and analyses to other observations

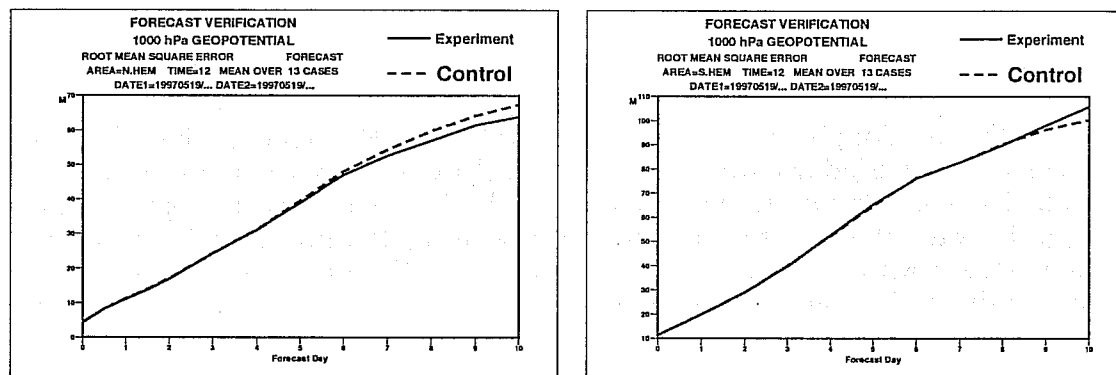
The first guess and analysis fits to the other observations were not significantly modified when SSM/I TCWV data were used in the assimilation except for radiosonde data and as expected TOVS water vapour channel radiances. When SSM/I 1DVar TCWV is assimilated the relative humidity analysis is biased slightly moist when compared to radiosondes in the Southern Hemisphere for both periods, which is consistent with the fact that the radiosondes are biased dry (cf. section 1). The rms fit of the analysis to the TOVS water vapour channel radiances is the same in both experiments, but as expected, the Experiment bias between analysis and observed TOVS radiances is different from the Control bias because the TOVS bias correction was not specifically updated for the Experiment run.

6 Forecast impacts

6.1 Forecast performance

The quality of the forecast when SSM/I TCWV data are used in 4DVar has been assessed by the comparison of root mean square (rms) error and anomaly correlation (not shown) for the 1000 hPa geopotential height averaged over the May'97 period and Dec'97 period (Fig. 8). The operational T213L31 ECMWF analyses have been used as the reference analyses for these computations. The forecast errors are shown for the Northern Hemisphere and Southern Hemisphere (poleward of 20°). In the Northern Hemisphere the rms errors are less for the May'97 period from day four and the same for the Dec'97 period. In the Southern Hemisphere the errors are the same for the May'97 period and slightly reduced from day three for the Dec'97 period. The use of SSM/I TCWV has more of an effect on the geopotential scores in the lowest part of the atmosphere. The rms errors of the 500 hPa geopotential height (not shown) are slightly higher where they are the same at 1000 hPa (from day four for the May'97 period in the Southern Hemisphere and from day five for the Dec'97 period in the Northern Hemisphere) and remain lower where they are lower at 1000 hPa. The forecast performance of the Experiment over Europe (not shown) is not significantly different from the Control.

a) May'97 period



b) Dec'97 period

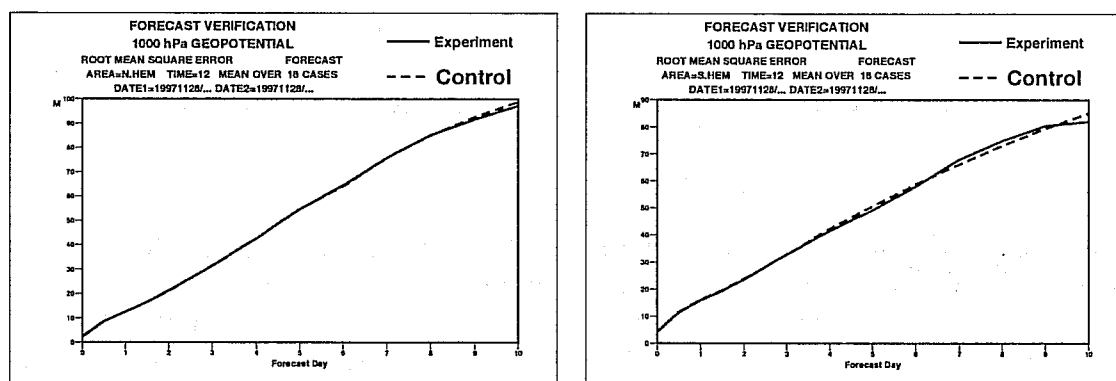


Figure 8: Root mean square error for forecasts from the Experiment (solid line) and the Control (dashed line), averaged over the May'97 period (a) and Dec'97 period (b). Errors are shown for geopotential height at 1000 hPa for the Northern Hemisphere (left panels) and the Southern Hemisphere (right panels).

The 200 hPa and 850 hPa vector wind scores in the Tropics (not shown) were computed against their own analysis, as the tropical analyses in the Experiments are significantly different from the operational ones. The effect of SSM/I TCWV data on the wind scores computed against their own analysis in the Tropics was slightly detrimental up to day three. This is because the additional moisture causes increased precipitation and associated latent heat release which can be detrimental to the wind field in the first few model time steps (see Section 6(c)). From day three SSM/I TCWV data help to reduce the rms error at 850 hPa for both periods. However when the vector wind root mean square errors are computed against the observations in the Tropics (Fig. 9) the results obtained with the Experiments are encouraging, as they are the same or slightly lower for both periods.

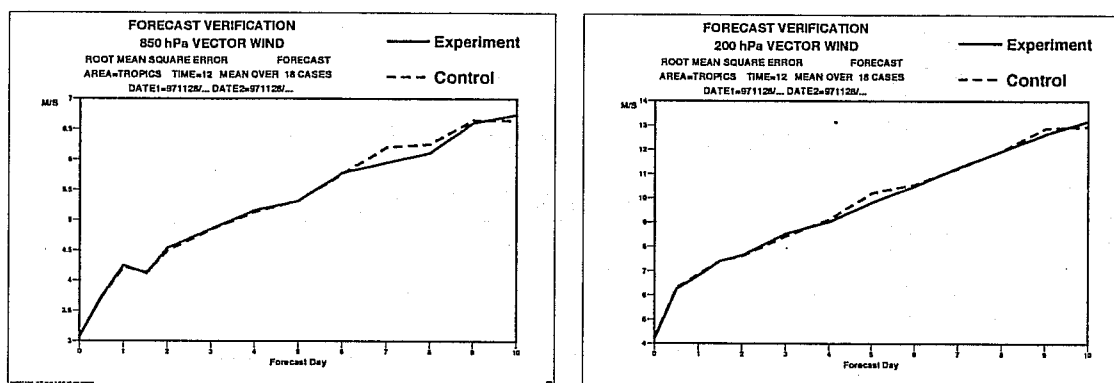


Figure 9: Root mean square error for tropical forecasts from the Experiment (solid line) and the Control (dashed line), averaged over the Dec'97 period. Errors are shown for vector wind at 850 hPa (left panel) and 200 hPa (right panel).

6.2 Impact on TCWV

The TCWV forecast fields from the Experiment have been compared to their verifying analyses to determine how different the forecast TCWV is from the analysis as a function of forecast range. The mean forecast minus analysis differences were checked to ensure there is a clear signal with low variability among the forecast cases. Fig. 10 shows the mean forecast minus analysis differences, for the Experiment for twelve cases of the Dec'97 period as a function of the forecast range up to day six. Fig. 10 also shows on the same plots how long the effect of assimilating SSM/I TCWV on the forecast lasts through the evolution of the average of TCWV forecast departure relative to the Control forecast. The influence of assimilating SSM/I TCWV remains in the forecasts for up to 3 days in the Southern Hemisphere but less in the Northern Hemisphere and Tropics. These results are similar for the May'97 period (not shown).

The evolution of the mean forecast TCWV errors has two regimes which are common to both experiments. The forecasts initially become significantly drier than the analysis during the first six hours and then become slowly moister during the medium range forecast in the Northern Hemisphere for both periods. The drying during the first 6 hours is higher in the Experiment than in the Control due to the extra moisture from SSM/I that the model tries to remove during the first forecast steps due to a hydrological imbalance in the analysis. The Southern Hemisphere and Tropical forecasts remain drier than the analysis for all ranges in the

Dec'97 period but there is a moistening in the medium range in the Southern Hemisphere for the May'97 period. The biggest differences between forecast and analysed TCWV are seen in the midlatitude summer hemisphere (-1.0 kg m^{-2} at day 6 in May for the Northern Hemisphere and -1.5 kg m^{-2} at day 6 in December for the Southern Hemisphere). The difference in the Tropics is around -0.5 kg m^{-2} for both periods.

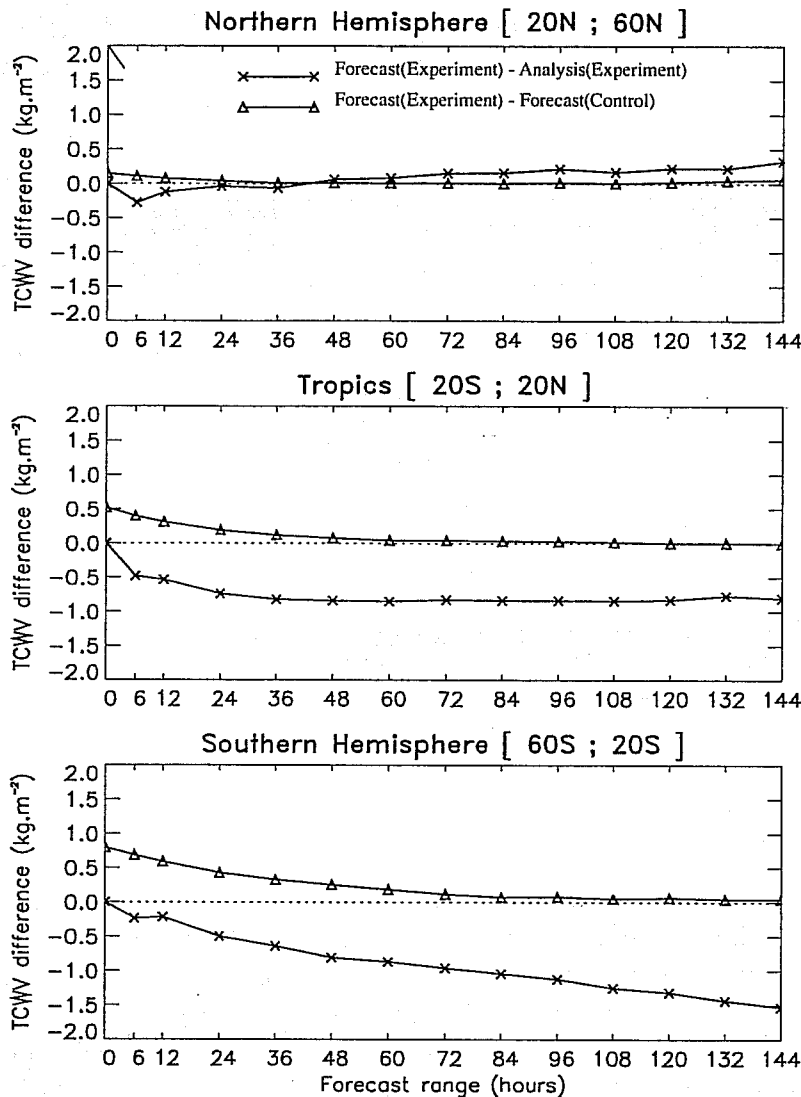


Figure 10: Mean TCWV forecast differences between the Experiment and Control forecasts (triangles) and mean difference between the Experiment forecasts and its own analyses (crosses) as a function of the forecast range, averaged over three latitude bands and over twelve forecasts of the Dec'97 period. Time step zero corresponds to analysis.

6.3 Impact on precipitation rate

The introduction of extra moisture provided by SSM/I in the assimilation also has a significant impact on the precipitation rate during the first forecast steps. Fig. 11 shows the mean precipitation rate over the May'97 period as a function of the forecast days up to day six for

the Northern Hemisphere, the Tropics and the Southern Hemisphere. For any latitude band the precipitation rate is greater in the Experiment than in the Control up to day two in the Northern Hemisphere and Tropics and up to day three in the Southern Hemisphere. After this time period the precipitation rate forecasts in both experiments are very similar. More precipitation occurs at the beginning of the forecast integration because more humidity is available in the analysis when SSM/I TCWV data are assimilated (see Fig. 3); the larger the TCWV analysis differences between the Experiment and the Control, i.e. in the Tropics and Southern Hemisphere, the bigger the impact on the precipitation rate forecast in the first model forecast steps.

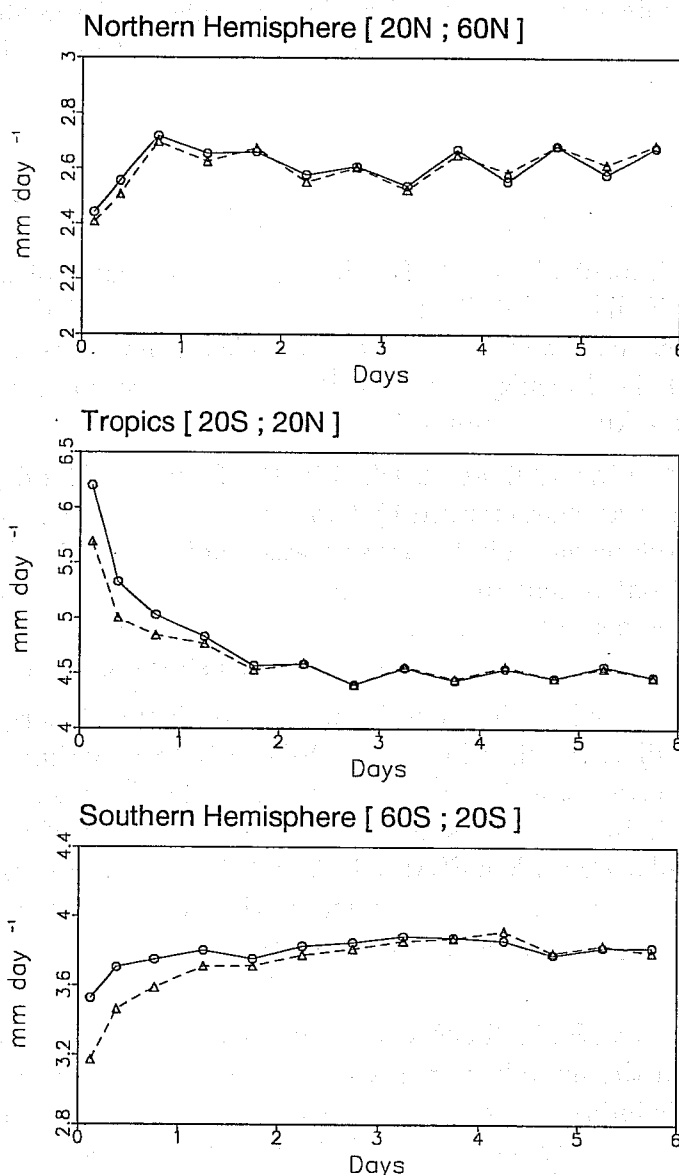


Figure 11: Evolution of precipitation rate forecast during forecast periods of up to six days, averaged over the May'97 cases, in the Northern Hemisphere (top panel), the Tropics (middle panel) and the Southern Hemisphere (bottom panel). The Control is shown as triangles on dashed line and the Experiment as circles on solid line.

The precipitation spin up of the Control in the Northern and Southern Hemispheres sug-

gests a lack of moisture at the beginning of the forecast. Adding SSM/I TCWV data in the analysis has a positive effect in these areas, as it reduces the precipitation spin up, especially in the Southern Hemisphere. On the other hand the precipitation spin down of the Control in the Tropics suggests that the increased moisture in the analysis is not consistent with the hydrological cycle in the model and needs to be removed through precipitation. This problem of increasing the forecast precipitation rates when assimilating SSM/I TCWV data in the Tropics is one obstacle to giving the data more weight in the assimilation.

The effect of SSM/I data on short range precipitation forecasts reveals how efficiently the TCWV is removed in the short-range forecast as shown by the TCWV increments in the Experiment which remain positive in the Tropics throughout the assimilation period. Fig. 3 demonstrates the inability of the model to retain all the moisture until the next assimilation cycle.

6.4 Case study

To investigate the impact of the SSM/I data on the forecasts of synoptic scale systems, forecasts from the Experiment and Control were studied to see if there were any differences between them. Only one case was found with a significant difference which is presented here. It must be emphasized the difficulty of identifying the exact reason for the improvement as is always the case for these kinds of studies.

This case was on 25 May 1997 at 12 UTC in the Southern Hemisphere at 60°S latitude when the synoptic scale was characterised by two low pressure systems at longitudes 20°E and 20°W. The forecast development of both systems was studied. Fig. 12 shows the mean sea level pressure maps of the Control and the Experiment at three forecast ranges, namely 5 days, 3 days and 1 day from the corresponding 12 UTC analyses 5, 3 and 1 day before 25 May 1997. The Control and Experiment verifying analyses are also shown on Fig. 12.

The two lows are analysed at the same location in both the Experiment and Control, and their intensities are similar, the first low is 971 hPa in both experiments and the second one at 949 hPa in the Experiment is 1 hPa deeper than in the Control. The comparison of the forecasts with their verifying analyses shows a more consistent set of medium and short range forecasts of this particular case when SSM/I 1DVar TCWV data are used in the assimilation. The forecasts of the low close to 25°E vary widely in the Control (differences of -16 hPa, 9 hPa and 5 hPa for day 5 to day 1 forecasts) but are more consistent in the Experiment (-5 hPa, 0 hPa and 3 hPa).

The positive impact of SSM/I TCWV data upon the forecasts is either due to a direct effect of SSM/I data on the humidity analysis increments which affect the dynamics through the forecast model, or is indirectly due to the rejection of other observations in the variational quality control. In this case it was observed that the short to medium range forecasts started from the analysis of the Control at 12 UTC advected 25% to 30% more moisture than in the Experiment forecasts. As a consequence the 72-hour forecast became 10 hPa deeper in the Control than in the Experiment, as more humidity was available in the Control than in the Experiment to intensify the low from the Brazilian coast towards the South-South-East. The exact reason for this was difficult to isolate as the moisture fields have gradually evolved into different states over the previous 10 days. There were no obvious differences in the use of data other than SSM/I TCWV for the analysis cycles immediately prior to the 12UTC analyses.

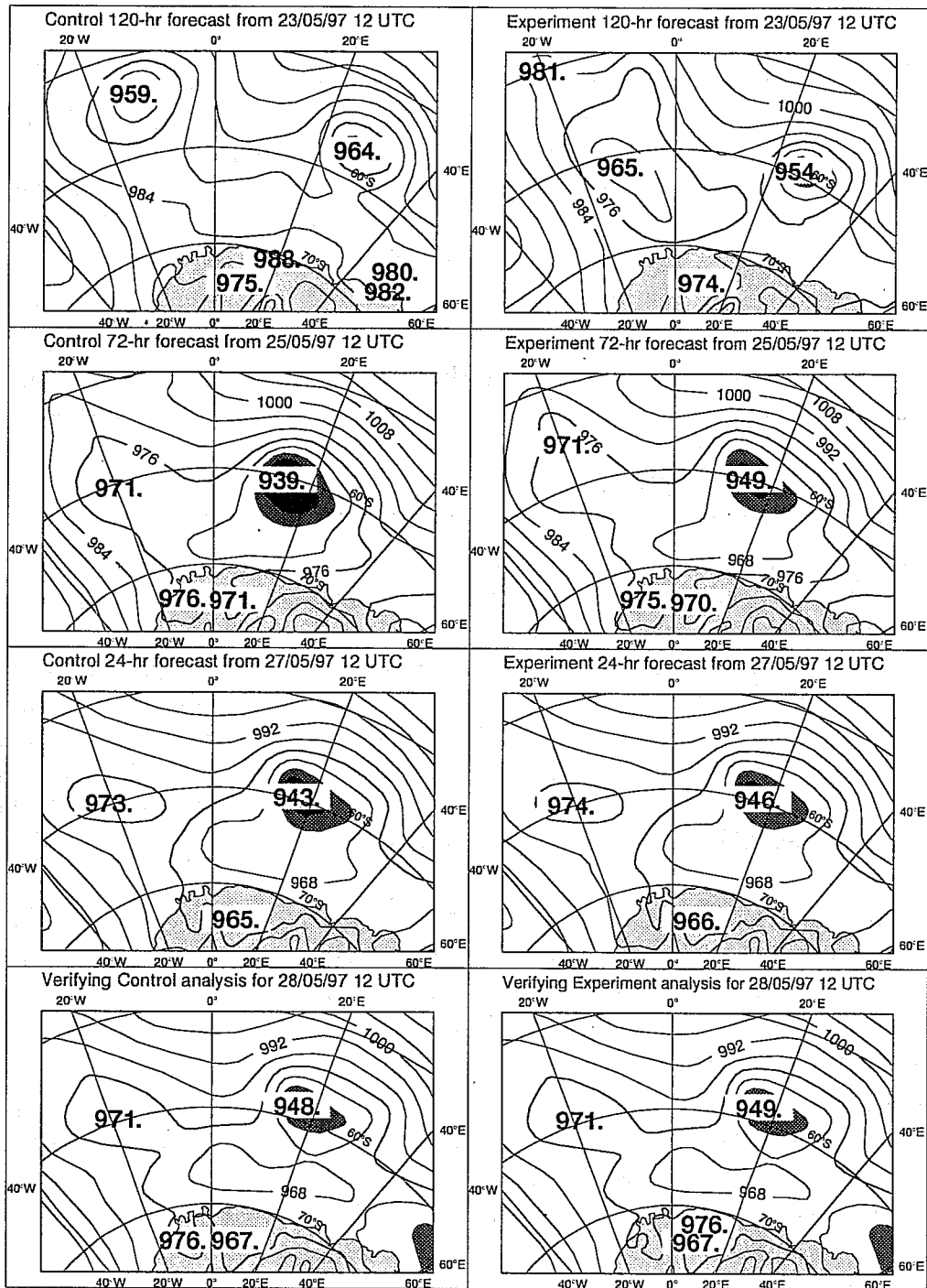


Figure 12: Mean sea level pressure maps showing the forecasts for two depressions in the Southern Hemisphere. The first three rows of panels from top to bottom show the 5-day, 3-day and 1-day forecasts respectively verifying 28 May 1997 at 12 UTC, and the bottom panels show the verifying analyses. Control charts are on the left, Experiment charts on the right. The contour intervals are 8 hPa.

7 Conclusions

The assimilation of SSM/I 1DVar TCWV in the ECMWF model modifies the analysed humidity fields by increasing the global water vapour amount by about 2%, particularly in the areas which are too dry, i.e. in the Tropics (2% increase) and Southern Hemisphere (4% increase). This is believed to be beneficial as it is known the radiosonde humidity profiles are biased dry and with the exception of HIRS water vapour channel radiances in cloudfree areas there are no other upper-air data to constrain the model humidity fields. The impact on the dynamics is to increase the strength of the Hadley circulation in the model.

The analyses which have assimilated SSM/I TCWV have demonstrated neutral to positive impacts on the Northern Hemisphere forecasts during two seasons. The impact on the Southern Hemisphere is dependent on the season, slightly positive in winter, neutral in summer. The forecast improvement is only seen in the lower part of the troposphere (below 500hPa). In the Tropics the wind forecasts are neutral when verified with observations. A case study shows that the intensities of two low pressure systems in the Southern Hemisphere were better forecast and their development detected earlier when SSM/I 1DVar TCWV data were used in the analysis.

In the Tropics and Southern Hemisphere, the hydrological cycle seems to be more active through the addition of extra-moisture from SSM/I in the assimilation. The precipitation rates are more intense during the first forecast steps, probably because the mixed layer depth does not change, whatever the amount of water vapour inserted in the lower part of the atmosphere, resulting in a rapid saturation of these layers. This inability of the model to retain the additional moisture in the tropics is one reason the SSM/I TCWV are only given a low weight (through specification of observation error) than might otherwise be appropriate. Developments in both the model physics and the data assimilation, through a better specification of the background errors for humidity should lead to a more optimal use of SSM/I TCWV and other humidity observations.

The computational cost of including the SSM/I 1DVar TCWV data at a sampling of 250km in the 4DVar observation vector was negligible. The 1DVar retrievals (sampling every 125 km) in the preprocessing added a few percent to the model run time. The SSM/I 1DVar retrievals of TCWV, surface wind speed and cloud liquid water path are computed and archived every 6 hours for model validation studies.

As a result of this study the assimilation of SSM/I TCWV from the DMSP F-13 satellite was introduced into the ECMWF operational system on 29 June 1998. The pre-operational parallel runs with SSM/I TCWV data and several other changes to the data assimilation confirmed the changes, reported here, to the analyses due to SSM/I when compared with the operational analyses.

It is planned to add the DMSP F-14 data in the future to enhance the coverage. Also the assimilation of the SSM/I 1DVar retrieved surface wind speed is now undergoing testing at ECMWF. A microwave imager similar to SSM/I is now in orbit on the Tropical Rainfall Measuring Mission (TRMM) referred to as TMI (TRMM Microwave Imager). It is planned to integrate TMI radiances within the SSM/I 1DVar framework to allow the possibility of assimilating TMI TCWV over the Tropics. Additional/different microwave frequencies on TMI provide, at least for the objective error estimation, an improved accuracy over SSM/I in terms of TCWV accuracy of about 20% (Mahfouf *et al.* 1998).

Acknowledgements

We thank NOAA for the provision of the SSM/I data in near real time. We also acknowledge the help given by the members of the Data Assimilation and Physics Sections at ECMWF in providing the necessary framework for this work and L. Phalippou for providing the initial version of 1DVar. Finally we are grateful for the guidance of A. Persson in helping to identify the case study.

References

- Alishouse, J. C., Snyder, S. A., Vongsathorn, J. and Ferraro, R. R., 1990: Determination of oceanic total precipitable water from the SSM/I. *IEEE Trans. Geosci. Remote Sensing*, **28**, 5, 811–816
- Andersson, E. and Järvinen, H., 1999: Variational quality control. *Q. J. R. Meteorol. Soc.*, **125**, (to be published)
- Aonashi, K. and Shibata, A., 1996: The impact of assimilating SSM/I precipitable water and rain flag data on humidity analysis and short-term precipitation forecasts. *J. Meteor. Soc. Japan*, **74**, 77–99
- Balagurov, A., Kats, A. and Krestyannikova, N., 1998: 'Implementation and results of the WMO radiosondes humidity sensors intercomparison - Phase I "Laboratory Test"'. Pp. 181–184 in Proceedings of the WMO technical conference on meteorological and environmental instruments and methods of observation (TECO-98), WMO instruments and observing methods report no. 70, Casablanca, Morocco, 13–15 May 1998
- Bauer, P. and Schuessel, P., 1993: Rainfall, total water, ice water and water vapour over sea from polarized microwave simulations and special sensor microwave/imager data. *J. Geophys. Res.*, **98**, 20737–20759
- Colton, M.C. and Poe, G.A., 1994: Shared processing program, DMSP, SSM/I Algorithm Symp., June 8–10, 1993. *Bull. Am. Meteorol. Soc.*, **75**, 1663–1669
- Deblonde, G., 1999: Variational assimilation of SSM/I total precipitable water retrievals in the CMC analysis system. *Mon. Weather Rev.*, (in press)
- Deblonde, G. and Wagneur, N., 1997: Evaluation of global numerical weather prediction analyses and forecasts using DMSP special sensor microwave imager retrievals. 1. satellite retrieval algorithm intercomparison study. *J. Geophys. Res.*, **102**, D2, 1833–1850
- Deblonde, G., Yu, W., Garand, L. and Dastoor, A. P., 1997: Evaluation of global numerical weather prediction analyses and forecasts using DMSP special sensor microwave imager retrievals. 2. Analyses/forecasts intercomparison with SSM/I retrievals. *J. Geophys. Res.*, **102**, D2, 1851–1866
- Eyre, J. R., Kelly, G. A., McNally, A. P., Andersson, E. and Persson, A., 1993: Assimilation of TOVS radiance information through one-dimensional variational analysis. *Q. J. R. Meteorol. Soc.*, **119**, 1427–1463
- Filiberti, M.-A., Rabier, F., Thépaut, J.-N., Eymard, L. and Courtier, P., 1998: Four-dimensional variational assimilation of SSM/I precipitable water content data. *Q. J. R. Meteorol. Soc.*, **124**, 1743–1770
- Gregory, D., Morcrette, J.-J., Jakob, C. and Beljaars, A., 1998: Introduction of revised radiation, convection, cloud and vertical diffusion schemes into Cy18r3 of the ECMWF integrated forecasting system. *ECMWF Technical Memorandum 254*
- Hollinger, J., Peirce, J. L. and Poe, G. A., 1990: SSM/I instrument evaluation. *IEEE Trans. Geosci. Remote Sensing*, **28**, 781–790
- Ledvina, D. V. and Pfendtner, J., 1995: Inclusion of SSM/I total precipitable water estimates into the GEOS-1 data assimilation system. *Mon. Weather Rev.*, **123**, 3003–3015

- Liebe, H. J., 1989: MPM - An atmospheric millimeter-wave propagation model. *Int. J. Infrared and Millimetre Waves*, **10**, 6, 631-650
- Lojou, J.-Y., Bernard, R. and Eymard, L., 1994: A simple method for testing brightness temperatures from satellite microwave radiometers. *J. Atmos. Oceanic Technol.*, **11**, 387-400
- McNally, A. P. and Vesperini, M., 1996: Variational analysis of humidity information from TOVS radiances. *Q. J. R. Meteorol. Soc.*, **122**, 1521-1544
- Mahfouf, J.-F., Gérard, É., Marécal, V., Miller, M. and Saunders, R., 1998: Requirements for the assimilation of TRMM products in the ECMWF 4D-Var system. *ECMWF Technical Memorandum 264*
- Offiler, D., Eymard, L., Kilham, D., Gérard, É. and Gäng, H., 1998: Cloud Retrieval Validation Experiment (CLOREVAL). Final Report to EU Contract No. ENV4-CT96-0302 (copy available from the National Meteorological Library, Bracknell, UK)
- Petty, G. W., 1990: 'On the response of the Special Sensor Microwave/Imager to the marine environment - Implications for atmospheric parameter retrievals'. PhD dissertation, University of Washington
- Phalippou, L., 1992: 'Comparison between SSM/I and ECMWF total precipitable water'. Pp. 22-26 in Proceedings of specialist meeting on microwave radiometry and remote sensing application. Ed. E. R. Westwater. Boulder, Colorado, June 1992
- Phalippou, L., 1993: A microwave radiative transfer model. *ECMWF Technical Memorandum 190*
- Phalippou, L., 1996: Variational retrieval of humidity profile, wind speed and cloud liquid water path with the SSM/I: Potential for numerical weather prediction. *Q. J. R. Meteorol. Soc.*, **122**, 327-355
- Phalippou, L. and Gérard, É., 1996: Use of precise microwave imagery in Numerical Weather Prediction. Study report to the European Space Agency, 1-70 (available from ECMWF)
- Rabier, F., Mahfouf, J.-F., Fisher, M., Järvinen, H., Simmons, A., Andersson, E., Bouttier, F., Courtier, P., Hamrud, M., Haseler, J., Hollingsworth, A., Isaksen, L., Klinker, E., Saarinen, S., Temperton, C., Thépaut, J.-N., Undén, P. and Vasiljević, D., 1997: Recent experimentation on 4D-Var and first results from a simplified Kalman filter. *ECMWF Technical Memorandum 240*
- Rabier, F., McNally, A., Andersson, E., Courtier, P., Undén, P., Eyre, J., Hollingsworth, A. and Bouttier, F., 1998: The ECMWF implementation of three-dimensional variational assimilation (3D-Var). II: Structure functions. *Quart. J. Roy. Meteor. Soc.*, **124**, 1809-1829
- Ritchie, A. R., Smith, M. R., Goodman, H. M., Schudalla, R. L., Conway, D. K., LaFontaine, F. J., Moss, D. and Motta, B., 1998: Critical analyses of data differences between FNMOC and AFGWC spawned SSM/I datasets. *J. Atmos. Sci.*, **55**, 1601-1621
- Rodgers, C. D., 1976: Retrieval of atmospheric temperature and composition from remote sensing of thermal radiation. *Rev. Geophys. Space Phys.*, **14**, 609-624
- Schmidlin, F. J., 1998: 'Summary of the WMO international radiosonde relative humidity sensor comparison - Sep, 1995 - Phase II "Field Test"'. Pp. 185-187 in Proceedings of the WMO technical conference on meteorological and environmental instruments and methods of observation (TECO-98), WMO instruments and observing methods report no. 70, Casablanca, Morocco, 13-15 May 1998

- Stoffelen, A. and Anderson, D., 1994: The ECMWF contribution to the characterisation, interpretation, calibration and validation of ERS-1 scatterometer backscatter measurements and winds, and their use in numerical weather prediction models. Final Report to ESA Contract No. 9097/90/NL/BI
- Vesperini, M., 1998: Humidity in the ECMWF model: Monitoring of operational analyses and forecasts using SSM/I observations. *Q. J. R. Meteorol. Soc.*, **124**, 1313–1327
- Wu, W. S. and Derber, J. C., 1994: 'Inclusion of SSM/I precipitable water observations in the NMC spectral statistical-interpolation analysis system'. Pp. 190-191 in Proceedings of the 10th AMS conference on numerical weather prediction, Portland, Oregon, July 1994